

Sensors Characterization for a Calibration-Free Connected Smart Insole for Healthy Ageing

Original

Sensors Characterization for a Calibration-Free Connected Smart Insole for Healthy Ageing / Gioacchini, Luca; Poli, Angelica; Cecchi, Stefania; Spinsante, Susanna. - STAMPA. - IoT Technologies for HealthCare:(2021), pp. 35-54. (International Conference on IoT Technologies for HealthCare Viana do Castelo, Portugal December 3, 2020) [10.1007/978-3-030-69963-5_3].

Availability:

This version is available at: 11583/2944974 since: 2022-02-21T15:50:52Z

Publisher:

Springer International Publishing

Published

DOI:10.1007/978-3-030-69963-5_3

Terms of use:

This article is made available under terms and conditions as specified in the corresponding bibliographic description in the repository

Publisher copyright

Springer postprint/Author's Accepted Manuscript (book chapters)

This is a post-peer-review, pre-copyedit version of a book chapter published in IoT Technologies for HealthCare. The final authenticated version is available online at: http://dx.doi.org/10.1007/978-3-030-69963-5_3

(Article begins on next page)

Sensors Characterization for a Calibration-Free Connected Smart Insole for Healthy Ageing ^{*}

Luca Gioacchini^[0000-0001-8258-8626]¹, Angelica Poli^[0000-0003-2600-4037]²,
Stefania Cecchi^[0000-0002-9625-814X]², and Susanna
Spinsante^[0000-0002-7323-4030]²

¹ Department of Electronics and Telecommunications, Politecnico di Torino, Torino
10129, Italy

`s257076@studenti.polito.it`

² Department of Information Engineering, Università Politecnica delle Marche,
Ancona 60131, Italy

`{a.poli, s.cecchi, s.spinsante}@staff.univpm.it`

Abstract. The design of technological aids to assist older adults in their ageing process and to ensure proper attendance and care, despite the decreasing percentage of young people in the demographic profiles of many developed countries, requires the proper selection of sensing components, in order to come up with devices that can be easily used and integrated into everyday life. This paper addresses the metrological characterization of pressure sensors to be inserted into smart insoles aimed at monitoring the older adult's physical activity levels. Two types of sensing elements are evaluated and a recommendation provided, based on the main requirement of designing a calibration-free insole: in this case, the pressure sensor should act as a switch, and the FSR 402 Short sensing element appears to be the proper solution to adopt.

Keywords: Smart Insole · Force Sensing Resistor · Step Counter · Healthy Ageing.

1 Introduction

In the last years, world population has undergone a demographic transition, in which the mortality and the birth rates both decreased. This means that globally, world population is shifting from a young age structure towards an old age one. The number of elders, especially in developed and wealthy countries, has increased and is now 10% higher than the number of young people. Because of the illnesses that inevitably appear after a certain age, or simply because the

^{*} Supported by the European Union's Active Assisted Living Programme under grant agreement AAL2017-63-vINCI, and the Italian Ministero dell'Istruzione, Università e Ricerca (CUP: I34I17000010005) within the project *vINCI*: "Clinically-validated INtegrated Support for Assistive Care and Lifestyle Improvement: the Human Link" (<https://vinci.ici.ro/>). Authors wish to thank the project partner Optima Molliter Srl for the provisioning of test devices.

physical resources dry out as people grow old, at some point older adults may find themselves in need for attendance and caring. But, due to the demographic ageing, there are fewer and fewer young people who can assist the older ones. This is the reason why there is a great need for an extra helping hand, something that can *aid both the elderly and the people who take care of them*. This huge help can be achieved through so called *assistive technology* (AT).

Research projects like vINCI [12] address the situation, aiming at designing the technological support that the elders and their caregivers need. Its purpose is to integrate different devices needed to monitor and improve the older adult's life, in a single, unifying platform. Moreover, it targets to enhance and sustain active aging of older adults, with devices like smart watches, smart insoles, monitoring cameras, together with tablets and properly designed software applications, which can be differently combined and composed according to the user's needs and preferences. In order to reach these goals, certain technical requirements must be met, either at the device and the cloud platform level. Not only devices must be able to connect to the platform and send data in a proper and recognized format, but also the cloud needs to be available all the time to prevent any data loss and to satisfy the users that interact with the dashboards or applications. All the interfaces need to be user-friendly and intuitive, especially because the users consists of older people who can be not very familiar with technology.

Among the requirements pertaining to the devices connected to the monitoring platform, a specific one refers to smart insoles [1], like those shown in Fig.1. These are wearable devices, connected over a Bluetooth Low Energy (BLE) link to a smartphone or eventually equipped with a long-range communication interface [10], which can be easily inserted into a user's common shoes, and they allow to count the steps performed in a day, and to recognize different motion statuses, such as walking, standing, sitting or not wearing the insole [5, 11]. According to the World Health Organization (WHO) guidelines about physical activity (PA)



Fig. 1. Smart insoles prototypes developed within the vINCI project.

in the older age [9], the amount of steps performed by an older adult in a day is a very important indicator of their physical and mental health status [7, 6]. In order to have devices that can be easily used by older adults, without the need for complex calibration processes, like those typically requested by smart insoles designed for sport and fitness purposes, a calibration-free design must be targeted. In fact, we aim for a device which is not expected to estimate the walked distance or the amount of burnt calories but, surprisingly, such a smart insole is currently not available in the market. As a consequence, this paper addresses the technical design of the smart insoles, specifically focusing on the proper selection of the sensing elements, which should allow to fulfill the expected aims avoiding the need for calibrating the subject’s walking profile. The main contribution of this paper is the metrological characterization of two different types of pressure sensors, in order to identify the most suitable solution for the design of a durable smart insole able to provide reliable data about the user’s PA, despite not requiring the calibration of the device by the user.

The paper is organized as follows: Section 2 shortly reviews the state-of-the-art about sensorized insoles for physical activity monitoring. Section 3 presents the design of the sensing insole, including motivations and sensors selection. Materials and methods for sensors characterization are presented in Section 4, while Section 5 presents and discusses the results obtained, under different conditions and analyses. Finally, Section 6 concludes the paper.

2 Background

Looking at the recent results about the design of smart insoles and in-shoe sensor systems, it appears that most of the studies are aimed at specific applications with clinical outcomes, such as gait analysis, real-time estimation of temporal gait parameters, foot motion analysis, and health monitoring.

Tahir et al. [13] discuss the growing interest in developing smart insoles associated to gait analysis, to be exploited in rehabilitation, clinical diagnostics and sport activities applications. Specifically, vertical Ground Reaction Forces (vGRF) and other gait variables could be measured by suitably designed wearable devices, able to continuously monitor plantar pressure through embedded sensors converting it into an electrical signal that can be further processed and eventually transmitted. In applications having potential clinical impact, it is important to use calibrated sensors to provide reliable measurements. In the mentioned work, authors state that calibration approaches adopted by different teams required expensive instruments such as universal testing machines or infrared motion capture cameras. In contrast, authors propose a systematic design and characterization procedure for three different types of pressure sensors: force-sensitive resistors (FSRs), ceramic piezoelectric sensors, and flexible piezoelectric sensors that can be used for detecting vGRF in a smart insole. The FSR proves to be the most effective sensor among the three tested, for smart insole applications. Shoe-embedded sensors have potentially huge advantages for the design of wearable robotic devices aimed at locomotion-related applications. In [3], the

development of a pair of pressure-sensitive insoles based on opto-electronic sensors for the real-time estimation of temporal gait parameters is presented. The system is assessed relatively to both vGRF and progression, providing satisfactory results in tests of ground-level walking at two speeds involving ten healthy participants. Recent advances in research concerning smart socks and in-shoe systems for foot motion analysis and health monitoring are reviewed in [2]. The considered devices represent textile-based systems and pressure sensitive insole (PSI) systems, respectively. They are analyzed with respect to special medical applications, for gait and foot pressure analysis, in comparison to the Pedar system used in medicine and sports. This paper aims to provide readers with a detailed overview of the above mentioned devices, to possibly improve their design and functionality, and find new application areas.

Considering the design of a connected smart insole for healthy aging-related applications, previous papers from some of the co-authors [1, 10, 5, 11] mostly addressed the electronics components and the data transmission interface. In this paper, the focus is on the choice and characterization of the sensing elements to be inserted into the insole, targeting a calibration-free device. With respect to the state-of-the-art presented above and summarized in Table 1, the current work provides details about the behavior of two specific pressure sensors selected for a smart insole not aimed at clinical observation but at the monitoring of PA in older adults. Usability and avoidance of complex configuration procedures are the leading design criteria for the device.

Table 1. Summary of recent smart insoles development in the literature.

Research paper	Application and main results
Tahir et al. [13]	Wearable sensors employed to detect vertical ground reaction forces (vGRF) and other gait variables. The paper provides a systematic design and characterization procedure for three different pressure sensors: FSRs, ceramic piezoelectric sensors, and flexible piezoelectric sensors.
Martini et al. [3]	The development of a pair of pressure-sensitive insoles based on optoelectronic sensors for the real-time estimation of temporal gait parameters is presented.
Dragulinescu et al. [2]	Both textile-based and pressure sensitive insole (PSI) systems are analyzed with respect to special medical applications, for gait and foot pressure analysis.

3 Design of the Sensing Insole

3.1 Motivations

The decision to address the design of a smart insole for the aims of the vINCI project purposes, was motivated by the fact that, performing a deep and careful

analysis of the devices available in the market, a few potential candidates were found, which were however not suitable for the project.

As a matter of fact, commercial devices such as Digitsole smart insole (<https://www.digitsole.com/>) or Moticon sensor insole (<https://www.moticon.de/>) are designed for runners and people interested in monitoring their performances during physical activities. In order to do so and to estimate, among others, the distance covered during a run or in general during the whole day just by walking, these devices typically require a *calibration procedure* with the user running on a treadmill, at different paces, for specific amount of time. For example, in the case of the insoles sold by Digitsole, the user is recommended to take about 200 steps at a fast pace so that the soles can analyze how he/she runs. The calibration shall be completed for a more detailed analysis of the strokes, as it allows the insoles to better understand the runner profile and therefore to more effectively measure the subsequent performance. Such a calibration, joint with details about height, weight, gender and age of the subject, provided through a specific app designed on purpose for the device, also enables the estimation of the amount of calories burnt by a subject, over a given period of time. It would not be possible for many older adults to perform such a type of calibration process. In general, this could be a barrier to the use of the smart insole by older customers, as addressed by the project.

For these reasons, we aimed at designing a smart insole that can enable the unobtrusive monitoring of the physical activity performed by an older adult, without requiring a calibration process. Of course, this choice implies that some functionalities, such as the estimation of the walked distance and the amount of calories burnt will not be possible. However, taking into account the fact that PA in older adults is defined in a broader way than for younger subjects (consider, for example, the definition of *light activity* [14] by the National Health System in UK), the design of the device can be somehow simplified and made more acceptable by users. Specifically, the design was based on the use of Force Sensing Resistors (FSRs) as pressure transducers, to generate signals from which both the number of steps performed and the type of PA carried out can be attained. Accelerometers are not considered in a first design phase, aiming for the simplest data processing possible, leading to minimal hardware requirements.

3.2 Sensors selection

Two kinds of sensors were evaluated to identify the viable solution: the FSR 402 Short provided by Interlink Electronics, and the FlexiForce A301 provided by Tekscan.

FSR 402 Short This tiny device, based on the thick-film technology, is basically a resistor which allows to detect weight and pressure by changing its resistance value. The use of this sensor model is suggested for the majority of do-it-yourself (DIY) Arduino-based projects and applications. The sensor essential design shown in Fig.2(a) consists of two layers separated by a spacer.

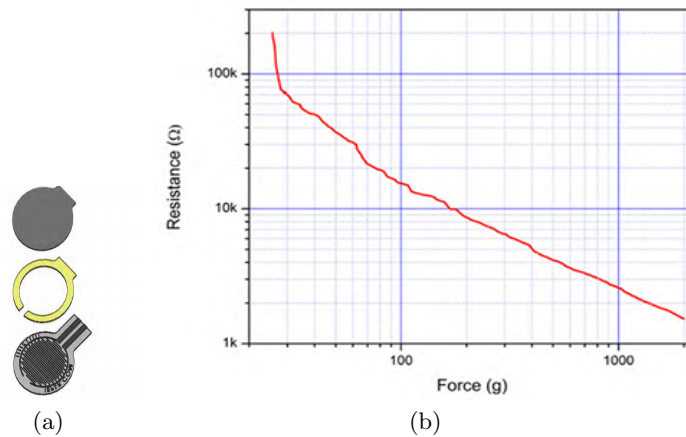


Fig. 2. (a) FSR 402 Short design. (b) FSR 402 Short Resistance/Force curve.

The upper layer (called FSR layer) is made of some flexible material such as PET or polyimide, coated with FSR carbon-based ink. The spacer has the double function of keeping together the two layers and maintaining the air gap. Its thickness is between 0.03 mm and 0.15 mm. The lower layer consists of a flexible polymer sheet such as polycarbonate or thin metal. It has also two sets of interdigitated traces. When the user applies a pressure on the bottom layer, the FSR ink shorts with the two tracks generating a variable resistance. The advantage of this technology is the increased miniaturization of the sensor provided by the incorporation of the passive element into the substrate. It allows a wide range of resistance with reasonable curing temperature, even if the resistance value becomes more unstable over the long period (especially with high temperature and humidity conditions). Interlink Electronics states that the force sensitivity range goes from 0.2 N to 20 N with a minimum of 0.2 N as actuation force. By using a repeatable actuation system, the repeatability of the single part is about $\pm 2\%$ of the initial reading. The long term drift ensured is $< 5\%$ per $\log_{10}(\text{time})$. This data is referred to 35 days of testing with 1 kg load. The hysteresis is $+10\%$ of the full scale. In Fig.2(b) the sensor resistance trend is shown, when the applied force changes. The actuation force is the one required to bring the sensor from the open circuit condition to below $100 \text{ k}\Omega$ resistance.

FlexiForce A301 Tekscan provides these piezoresistive sensors whose behavior is determined by *strain* and the *Hooke's Law*. The former is defined as the relative change in the shape or size of an elastic object due to an applied force. The latter states that the strain of an elastic object is directly proportional to the applied force. This way, it is clear that by measuring the physical changing of an object after the application of a force it is possible to measure the force itself. The most common device used for this purpose is an electrical resistance strain gauge, since the resistance of a conductor is directly proportional to its length and inversely

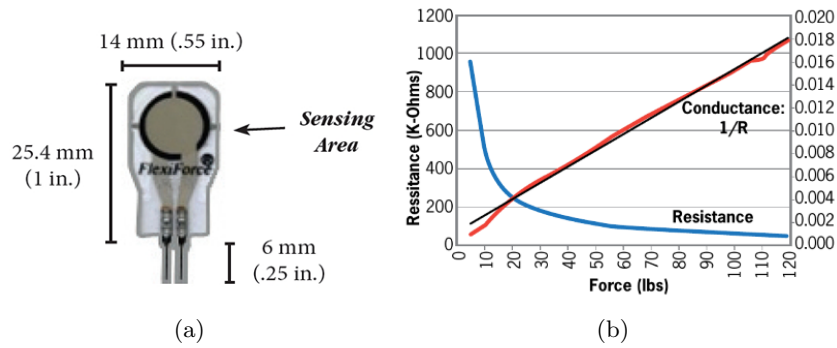


Fig. 3. (a) FlexiForce A301 design. (b) Resistance/Force and Conductance/Force trends for a 100lb FlexiForce A301 sensor (in black, an ideal linear dependency between force and output resistance).

proportional to its cross-sectional area:

$$R = \int_{\Delta L} \frac{\rho(l)dl}{S(l)} \quad (1)$$

where $\rho(l)$ is the electrical resistivity of the conductor, $S(l)$ is the cross sectional area and ΔL is the length variation of the conductor. If the resistance is attached to an elastic element, when it is modified, the resistance length changes too. As we can see in Fig. 3(b) the resistance has a non-linear trend with strain, so usually a linearization circuit is required.

Having clarified the basic principles, we have to consider that the A301 is made of a piezoresistive material located between two conductive layers. This particular material differs from a simply resistive one from the fact that its resistance depends on the force applied to the material, rather than its size change. Similar to the FSR sensor, the resistance of a piezoresistive one drops from several $M\Omega$ when no force is applied, to a few $k\Omega$ when pressed.

Tekscan provides three versions of this sensor: the first one can tolerate a maximum 4.4 N load, the second one a 111 N load, and the third one a 445 N load. By using a repeatable actuation system, the ensured repeatability is $\pm 2.5\%$ of the initial reading. The long term drift ensured is $< 5\%$ per $\log_{10}(\text{time})$, tested with a constant 111 N load. The hysteresis is $< 4.5\%$ of the full scale.

4 Materials and Method for Sensors Characterization

The measurement setup for sensor characterization is presented in this section. It consists of an Arduino UNO board with a voltage divider, a baropodometric platform and a software tool developed in Python to control the Arduino board, and allow the serial communication with the computer. Two main functions are implemented: the former enables the acquisition of a single resistance value and

it is used for a preliminary check of operation. The latter allows a continuous stream of data and plots them. The acquisition is stopped manually by the operator.

The role of the Arduino board is to acquire the variations of the sensor resistance originated by the pressure applied on it. Sensors are connected to the board through a voltage divider shown in Fig.4, where the variable resistance R_2 represents the sensor, whereas R_1 is a reference resistance of fixed value. This way, the variation of resistance is converted into a voltage signal to measure, named V_{out} , which is given by:

$$V_{out} = V_{in} \frac{R_2}{R_1 + R_2} \quad (2)$$

The reference voltage V_{in} is 5 V and it is taken directly from one of the Arduino pin. The V_{out} value is taken from an analog reading of the A0 pin of the board. The Arduino sampling frequency is 20 Hz and the ADC (Analog to Digital Converter) has a resolution of 10 bits. In order to get the sensor resistance value, the following equations are applied:

$$R_{sensor} = \frac{V_{in} - V_{out}}{V_{out}} \cdot R_1 \quad (3)$$

$$V_{out} = \frac{V_{in} \cdot V_{read}}{1024} \quad (4)$$

Where R_{sensor} is the resistance value of the sensor, V_{read} is the analog read voltage (it must be converted according to the Arduino ADC resolution: a 10-bit resolution involves a range of 1024 values), V_{out} is the real output tension and R_1 is the 10 k Ω reference resistance.

A fixed dynamometric platform (Bertec H4060) based on strain gauge technology is used as the reference measurement instrument [4], in such a way to have a calibrated and accurate measurement of the force applied on the sensor. Data from the platform are acquired by means of a professional movement analysis system (Elite, BTS-Bioengineering, Italy) with a sampling rate of 500 Hz.

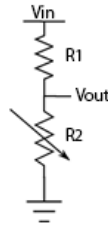


Fig. 4. Voltage divider used for the sensors characterization.

Two different experiment sessions were carried out: the former with heavy weights, the latter with light weights. Since we want to characterize force sensitive resistors, we need to know exactly how heavy is the applied load, and its distribution over the measuring devices. So, we used a 3 kg triangular medium shown in Fig.5 as a supporting tool to measure heavy weights, and a 0.6 kg wooden medium to help measuring light weights. Both of them were based on three rebars slightly smaller than the sensors sensitive areas. This way, by adding loads over the medium, we can be sure that the weight is evenly distributed on the sensor active area. The load consists of an increasing number of 10 kg and 1 kg weight plates for the first kind of data acquisitions, and an increasing number of 0.1 kg of water-filled elements in the range [0.1, 0.3] kg for the second one.

In order to get an accurate measurement of the force (in Newton) applied on the sensor we used the baropodometric platform (shown in Fig.5) for the high weights measurements and an electronic kitchen scale with resolution 1 gr for the low weights ones. This way it is possible to determine the resistance value in relation to the applied force. It is important to explain the measurement procedure when the baropodometric platform is used: at the beginning of each measurement, it is necessary to clear out the platform in order to measure the no-load offset. After that, the operator can put the load and start the measurement. Since Arduino and the force platform are stand-alone devices, as shown in Fig. 6, the trigger for their synchronisation was verbally determined by two

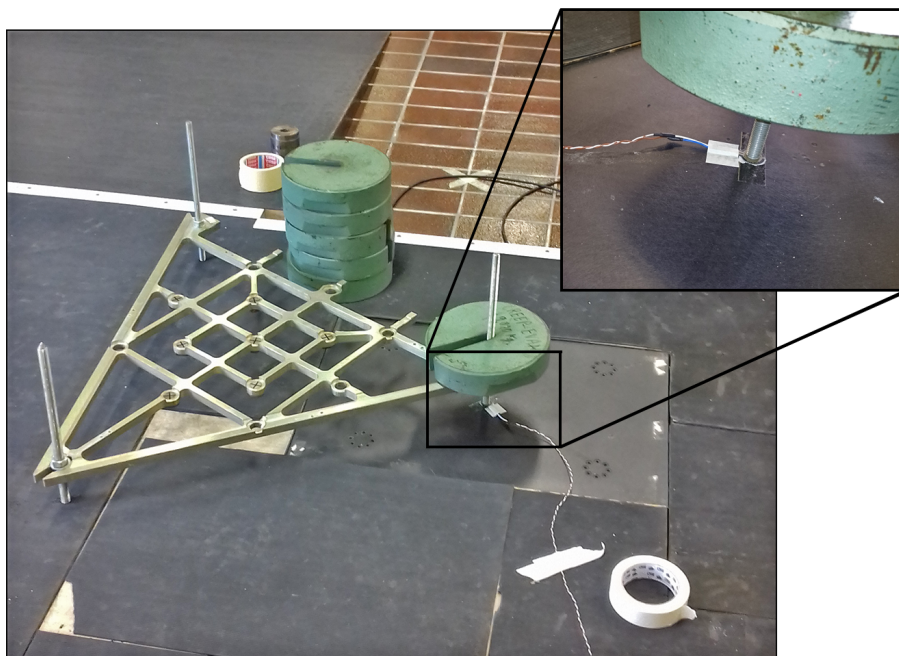


Fig. 5. Experimental measurement setup.

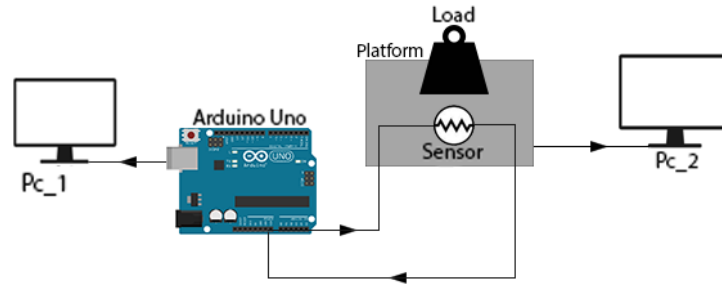


Fig. 6. Functional scheme of the measurement setup.

computer operators. The output of the takes is a pair of .dat files ready to be processed. Because of the different sampling frequencies of the two devices and the approximate vocal trigger for the acquisition, data should be downsampled to 20 Hz and the excess values should be discarded, to obtain a matrix without zeros.

5 Experimental Results and Discussion

In this section the experimental results about mean resistance values measurements are presented, as well as considerations relating to the drift phenomenon affecting the sensors under evaluation.

5.1 Sensors Characterization in the Case of High Weights

Mean Resistance/Force (R/F) Values Some first useful measurements are obtained as the mean values of the resistance assumed by the sensors during each measurement operation³.

In Fig.7 and Fig.8 the trend of the resistance values assumed by the FSR 402 Short and the relative scatter-plots obtained during two measurement sessions are reported. In Fig.9 and Fig.10 the same results are shown when the FlexiForce A301 is used.

As we can see from the plots in Fig.7 and Fig.9, by applying the 3 kg medium only on the sensors (i.e. performing an off-load measurement), none of them reaches the saturation condition, even if the FSR assumes a resistance value much lower than the FlexiForce one (0.68 k Ω compared with 225.58 k Ω).

By applying a load of about 13 kg⁴ on the devices, a different behavior of the sensors is observed. The 402 Short sensor enters its saturation zone: it takes on a 0.21 k Ω resistance value from which the following variations are very small,

³ E.g. three consecutive measurement operations are performed, by applying 12 N on the sensor, so the values plotted in Fig.7 are the mean of each measurement session.

⁴ 10 kg weight plate plus 3 kg of the supporting medium.

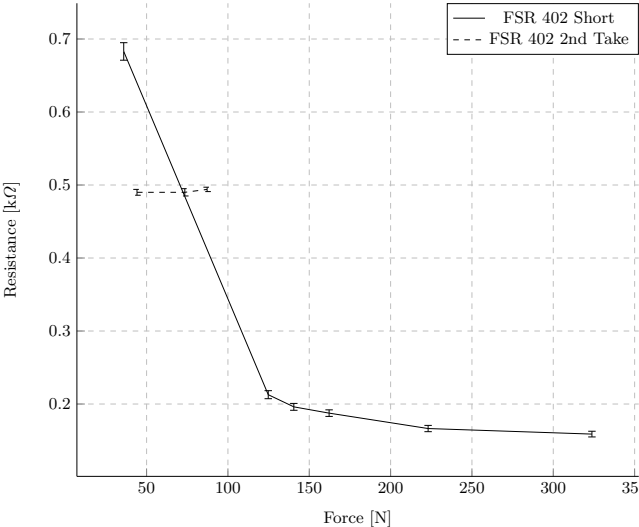


Fig. 7. FSR 402 Short force/resistance trend. Plotted values are the mean ones collected during the acquisitions. It is indicated the standard deviation of each value. The dashed line shows the resistance values obtained when 4.5 kg, 7.5 kg and 8.9 kg are applied in a second measurement session.

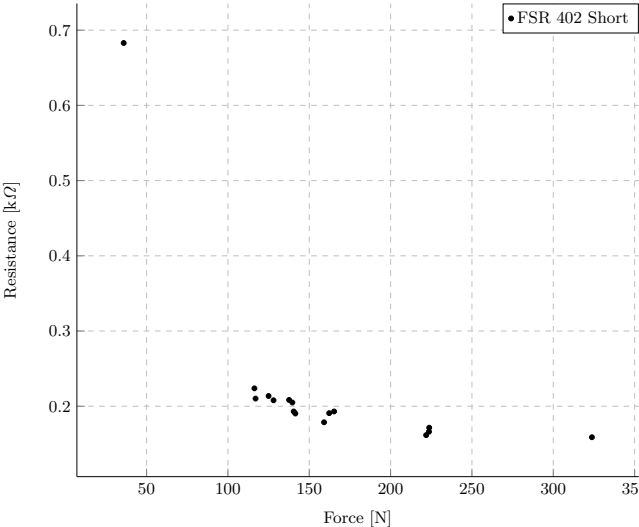


Fig. 8. Force/resistance values scatter plot of the FSR 402 Short sensor for the same applied load values of Fig.7.

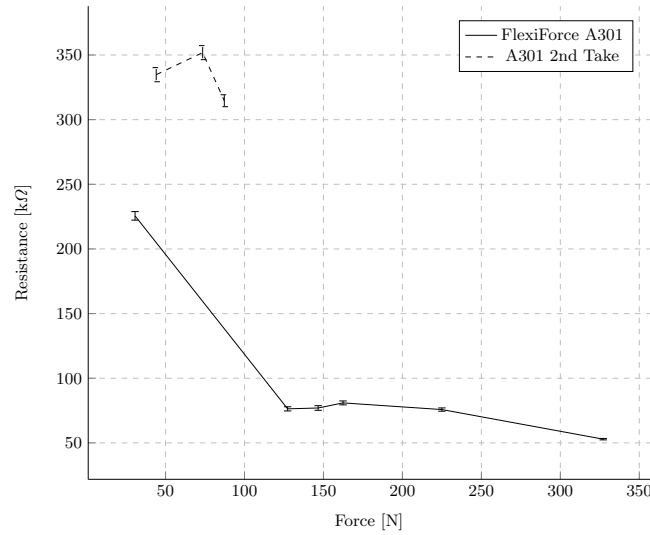


Fig. 9. FlexiForce A301 force/resistance trend. Plotted values are the mean ones collected during the acquisitions. It is indicated the standard deviation of each value. The dashed line shows the resistance values obtained when 4.5 kg, 7.5 kg and 8.9 kg load values are applied in a second measurement session.

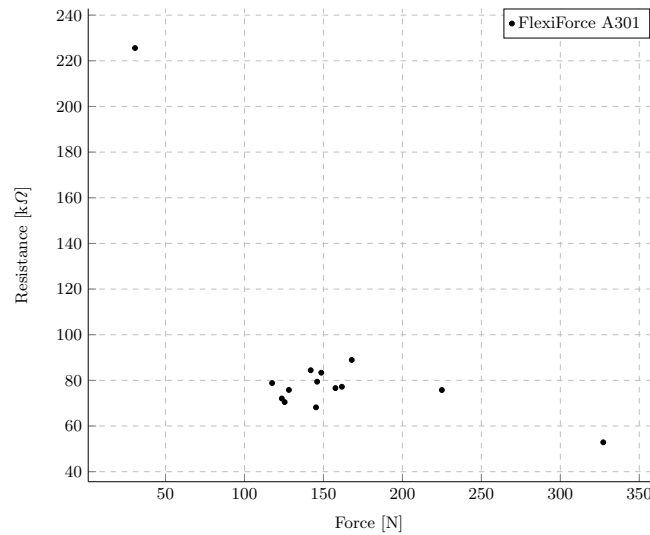


Fig. 10. Force/resistance values scatter plot of the FlexiForce A301 sensor for the same applied load values of Fig.9.

even when increasing the applied load. In fact, by adding an increased amount of weight, the measured resistance decreases a little, down to a *floor* of about $0.16 \text{ k}\Omega$. On the other hand, the A301 sensor, whose datasheet ensures a maximum load of 45 kg, is still in its linear working zone. As we can see from Fig.9, the R/F curve keeps a slight concavity and a little offset corresponding to the [13, 15] kg range. This means that the range of values assumed by the sensor is still wide, and not limited by the floor resistance value (by applying a 146.6 N load, a resistance value of $76.9 \text{ k}\Omega$ is obtained; for a 327.18 N load, the resistance value is $52.8 \text{ k}\Omega$). This is also confirmed by Fig.8, in which the value markers of each measurement are densely placed around the floor resistance value, while in Fig.10 they are more widespread.

The dashed lines of Fig.7 and Fig.9 show the resistance values assumed by the FSR 402 Short and the FlexiForce A301 sensors, respectively, when 4.5 kg, 7.5 kg and 8.9 kg are applied, during a different measurement session. Even if the resistance values exhibited by the 402 Short sensor are not representative of the general trend obtained during the first test, they lie within a range of values coherent with the other measurements. On the other hand, the resistance values provided by the A301 sensor are quite patchy. We can assume that this is because for this different measurement session we used a commercial balance, which is not so sensitive to the 0.1-fold weight variations. Furthermore, we changed the specific sensor devices under test (even if, of course, belonging to the same FSR 402 Short and FlexiForce A301 families). This means that each sensor item is more or less sensible to weight variations, so it would always request an a priori calibration, if aimed at *measuring* the force value applied. We need also to observe the position of the supporting medium on the sensors' active areas. In fact, if the medium is barely located on the A301 spacer, this can affect the weight distribution, causing a possible resistance value shift of up to $100 \text{ k}\Omega$.

Drift Evaluation Another useful data for a sensor characterization is the drift factor. Considering the procedures used in [8], the drift analysis has been led through a 60 seconds-long static measurement when the sensors are in their linear working zone, so when the 3 kg medium only is applied on the FSR 402 Short, and when a 20 kg-weight plate plus the 3 kg medium is located on the A301 sensor. Measuring the initial and final value of the resistance, given by R_i and R_f , respectively, the percent drift of the resistance value (D_R) is calculated as:

$$D_R = 100 \cdot (R_f - R_i)/R_i \quad (5)$$

Fig.11 and Fig.12 provide a qualitative information about the sensors' drift reporting the resistance values oscillations and decreasing exhibited by the sensors during the constant weight application.

Even if the A301 resistance floats over a greater number of different values, after 60 seconds (i.e. 1200 samples), the drift factor is about the 6.94% of the initial value. This is lower than the FSR 402 Short one, which is about the 10% of the initial value, as shown in Fig.11.

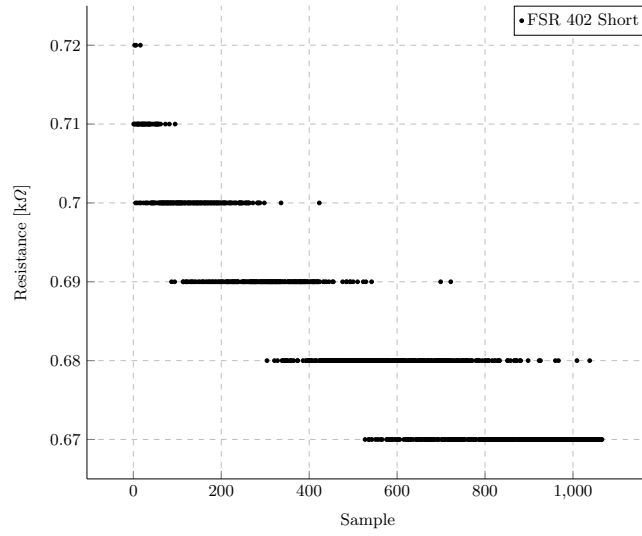


Fig. 11. Scatter plot of the FSR 402 Short sensor when the 3 kg medium is statically applied for a time of 60 s, aimed at its drift analysis.

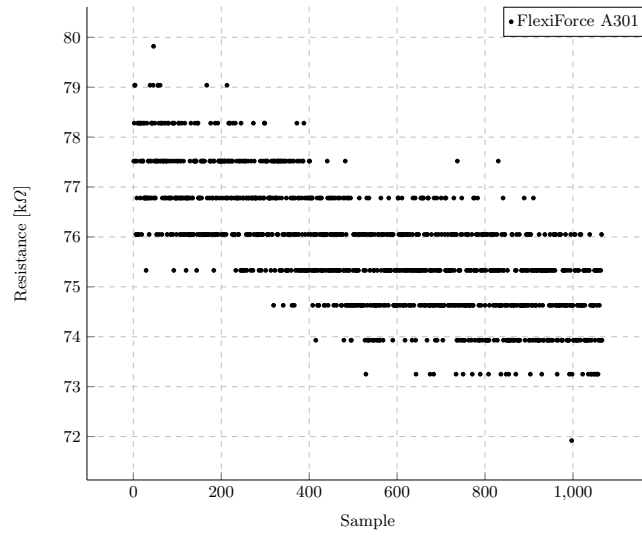


Fig. 12. Scatter plot of the FlexiForce A301 sensor when the 23 kg are applied for 60 seconds for a drift analysis.

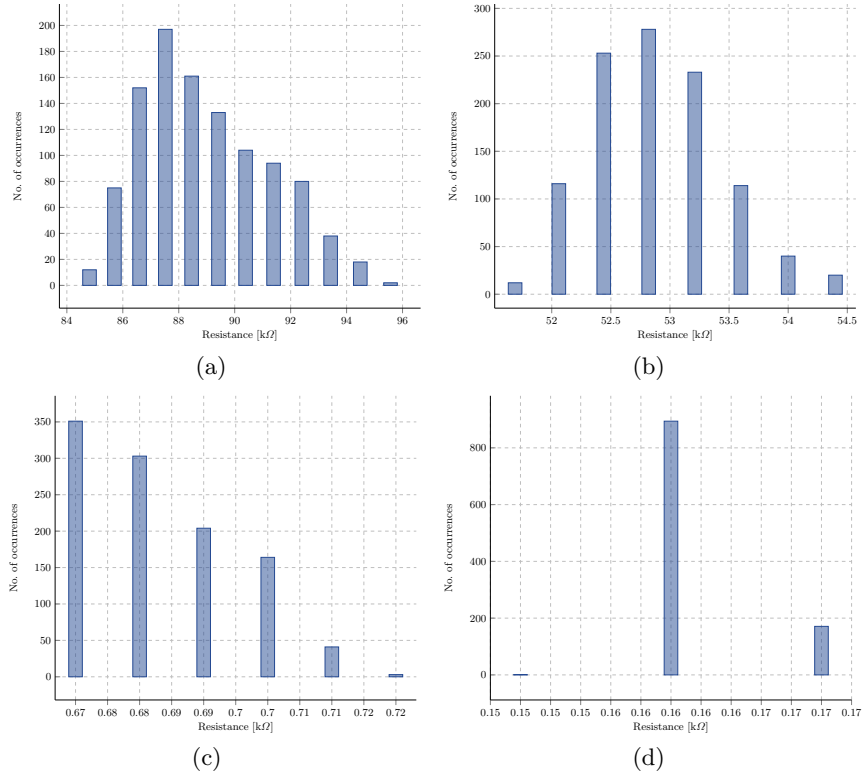


Fig. 13. Comparison between resistance values distributions: (a) A301 with 23 kg applied, linear working zone; (b) A301 with 33 kg applied, linear working zone, but near to the saturation one; (c) 402 Short with 3 kg applied, linear working zone, but near to the saturation one; (d) 402 Short with 13 kg applied, entering the saturation working zone.

By considering that both datasheets ensured a drift factor $<5\%$ of the initial value, it is clear that the FlexiForce sensor is not so far from this condition, while the FSR one has a quite different performance. Another consideration is necessary. By calculating the mean drift factor of all the acquisition takes for each sensor, it results that the 402 Short sensor has a drift factor equal to the 3.33% of the initial value, while the A301 one is about the 5.22% of the initial values. This results seem to conflict with all the previous considerations. However it should be noticed that during most of the measurements the FSR worked in its saturation zone, so, as far as a constant weight is applied, its resistance value cannot be lower than the floor one. Therefore, it is clear that the drift factor will certainly be lower than the A301 one, which works in linear zone and can assume a wider range of value.

To investigate the distributions of the resistance values assumed by the sensors, Fig.13 show the values frequency of the A301 and FSR 402 in linear working zone and when the saturation one is approached. In all the cases, by gradually approaching the saturation working zone, the amount of values the sensors' resistance can assume decreases. When the weight applied on the A301 is 23 kg, the sensor resistance floats among 12 values (Fig.13(a)). In Fig.13(b) the weight applied is about 33 kg. By remembering that the maximum admitted weight for this sensor is 45 kg, we are approaching the saturation working zone, so the number of values assumed by the resistance goes down to 8. By applying about 3 kg on the FSR 402 sensor (Fig.13(c)), we are in a border working zone, so the number of assumed resistance values is 6. When a 13 kg weight it is applied on it (Fig.13(d)), this number decreases even further, to 3 values, floating around the floor. In view of this, data is consistent with what has been observed before.

5.2 Sensors Characterization in the Case of Low Weights

Very different results are obtained from the low weights measurements as it can be seen from the trend and scatter plot of Fig.14 and Fig.15 for the FSR 402. In this case the sensors exhibit a reverse behaviour: the FSR 402 Short seems to be more sensitive to the 0.1-fold weight variations. As it is shown in Fig.14 and Fig.15, except for a little offset when 2.1 kg and 2.2 kg are applied, the Force/Resistance trend is more akin to the datasheet one, and the standard deviation is very small, so the resistance values are quite accurate. Furthermore, when 2.9 kg are applied on the sensor, its resistance value is about $1.032\text{ k}\Omega$, which, according to what we have said at the end of Section 5.1, after a previous calibration, should be easily led to $0.68\text{ k}\Omega$ of the Fig.7. By observing the plots in Fig.16 and Fig.17, in which the resistance values trend and scatter plot for the FlexiForce are reported, it is clear that the A301 sensor is not very sensitive to low weights variations. In fact, it does not work until 0.5 kg are applied on it. After that threshold, the resistance values don't have an identifiable pattern and the standard deviation values are greater than in the other cases. This means that after 30 seconds of acquisition, the resistance values float between a certain value and zero. We can explain this behaviour by the fact that the activation

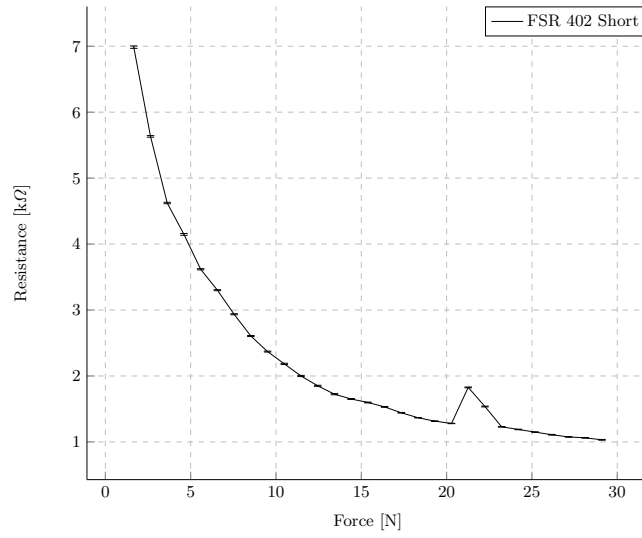


Fig. 14. Low weight FSR 402 Short Force/Resistance trend. Plotted values are the mean ones collected during the acquisitions. The standard deviation of each value is also reported.

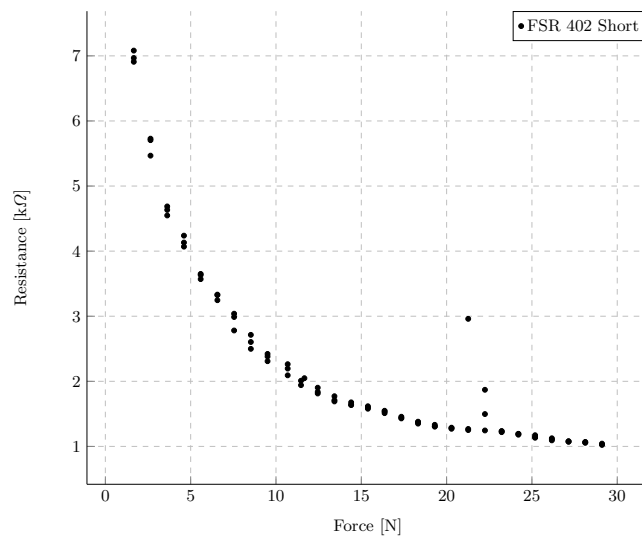


Fig. 15. Low weights Force/Resistance values scatter plot of the FSR 402 Short sensor.

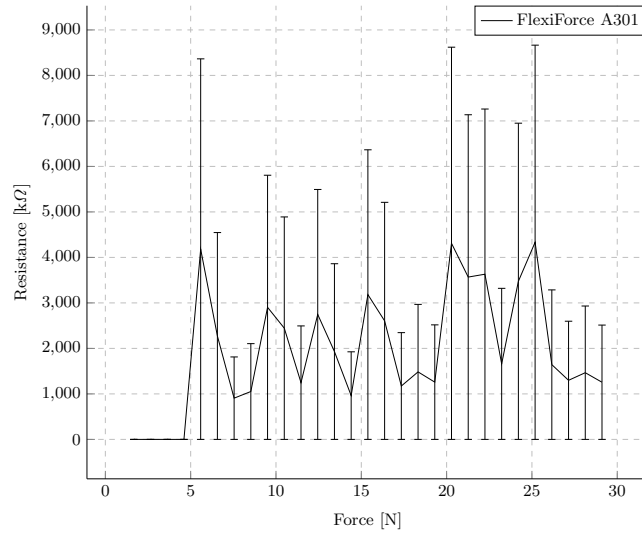


Fig. 16. Low weight FlexiForce A301 Force/Resistance trend. Plotted values are the mean ones collected during the acquisitions. The standard deviation of each value is also reported.

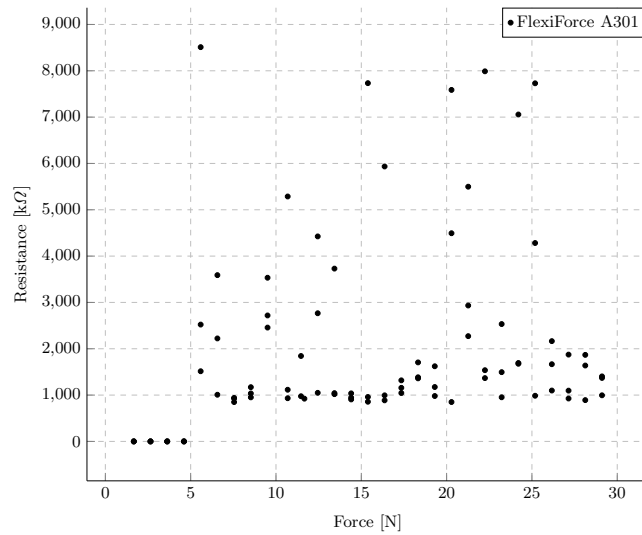


Fig. 17. Low weights Force/Resistance values scatter plot of the FlexiForce A301 sensor.

force of this sensor has not been reached yet, and so, over the long term, it exhibits an unstable output.

6 Conclusion

Following the results presented above, two kinds of applications may be targeted by the examined sensors: those exploiting the sensor as a switch, and those which use it as an indicator of the weight applied. The specific devices tested may be recommended for the first kind of applications. In fact, after having selected a certain threshold, based on the calibration results performed in the lab on each sensor item, the random floating of the attained resistance values becomes irrelevant to the application. Then, the sensor to use should be selected based on the expected load and the supported range. As far as the second kind of application is concerned, A301 sensors are recommended for high weights and the FSR 402 Short for the low ones, especially for touch-based interaction applications, thanks to the high sensitivity of the device. Based on these findings, the FSR used in the first insole prototype design was the FSR 402 Short, to detect, by means of a proper software application running on the embedded board, the three different activity statuses mentioned before. The raw sensor measurements are not transmitted; the information about the status is generated onboard, by processing locally the raw sensor measurements. Transmissions from the insole take place only at a status change, and whenever the step counter increases. As a future development of the smart insole design, it is foreseen to integrate the FSR data with acceleration measurements, in order to improve the PA detection, the classification of the activity performed, and, possibly, to implement the evaluation of the covered distance within a day.

Acknowledgment

Authors wish to thank Dr. Federica Verdini from the Information Engineering Department at the Marche Polytechnic University for her help in collecting measurements from the baropodometric platform available at the Movement Analysis Bioengineering Lab.

References

1. De Santis, A., Gambi, E., Montanini, L., Raffaelli, L., Spinsante, S., Rascioni, G.: A simple object for elderly vitality monitoring: The smart insole. In: 2014 IEEE/ASME 10th International Conference on Mechatronic and Embedded Systems and Applications (MESA). pp. 1–6 (2014)
2. Drăgulinescu, A., Drăgulinescu, A.M., Zincă, G., Bucur, D., Feieș, V., Neagu, D.M.: Smart Socks and In-Shoe Systems: State-of-the-Art for Two Popular Technologies for Foot Motion Analysis, Sports, and Medical Applications. *Sensors* **20**(15) (2020). <https://doi.org/10.3390/s20154316>, <https://www.mdpi.com/1424-8220/20/15/4316>

3. Martini, E., Fiumalbi, T., Dell'Agnello, F., Ivanić, Z., Munih, M., Vitiello, N., Crea, S.: Pressure-Sensitive Insoles for Real-Time Gait-Related Applications. *Sensors* **20**(5) (2020). <https://doi.org/10.3390/s20051448>, <https://www.mdpi.com/1424-8220/20/5/1448>
4. Mengarelli, A., Cardarelli, S., Tigrini, A., Fioretti, S., Verdini, F.: Kinetic data simultaneously acquired from dynamometric force plate and nintendo wii balance board during human static posture trials. *Data in Brief* **28**, 105028 (2020). <https://doi.org/https://doi.org/10.1016/j.dib.2019.105028>, <http://www.sciencedirect.com/science/article/pii/S2352340919313848>
5. Montanini, L., Del Campo, A., Perla, D., Spinsante, S., Gambi, E.: A footwear-based methodology for fall detection. *IEEE Sensors Journal* **18**(3), 1233–1242 (Feb 2018). <https://doi.org/10.1109/JSEN.2017.2778742>
6. Mura, G., Mauro Giovanni, C.: Physical activity in depressed elderly. a systematic review. *Clinical Practice and Epidemiology in Mental Health* **9**, 125–135 (2013)
7. Nakamura, Y., Tanaka, K., Yabushita, N., Sakai, T., Shigematsu, R.: Effects of exercise frequency on functional fitness in older adult women. *Archives of Gerontology and Geriatrics* **44**(2), 163–173 (2007)
8. Parmar, S., Khodasevych, L., Troynikov, O.: Evaluation of flexible force sensors for pressure monitoring in treatment of chronic venous disorders. *Sensors* **17**(8) (2017). <https://doi.org/10.3390/s17081923>, <https://www.mdpi.com/1424-8220/17/8/1923>
9. Physical Activity Guidelines Advisory Committee (PAGAC): Physical activity guidelines advisory committee report, 2018. https://www.who.int/dietphysicalactivity/factsheet_olderadults/en/, online; accessed 03 October 2020
10. Spinsante, S., Poli, A., Pirani, S., Gioacchini, L.: Lora evaluation in mobility conditions for a connected smart shoe measuring physical activity. In: 2019 IEEE International Symposium on Measurements Networking (M N). pp. 1–5 (2019)
11. Spinsante, S., Scalise, L.: Measurement of elderly daily physical activity by unobtrusive instrumented shoes. In: 2018 IEEE International Symposium on Medical Measurements and Applications (MeMeA). pp. 1–5 (2018)
12. Spinsante, S., Strazza, A., Dobre, C., Bajenaru, L., Mavromoustakis, C.X., Batalla, J.M., Krawiec, P., Georgescu, G., Molan, G., Gonzalez-Velez, H., Herghelegiu, A.M., Prada, G.I., Draghici, R.: Integrated Consumer Technologies for Older Adults' Quality of Life Improvement: the vINCI Project. In: 2019 IEEE 23rd International Symposium on Consumer Technologies (ISCT). pp. 273–278 (2019)
13. Tahir, A.M., Chowdhury, M.E.H., Khandakar, A., Al-Hamouz, S., Abdalla, M., Awadallah, S., Reaz, M.B.I., Al-Emadi, N.: A Systematic Approach to the Design and Characterization of a Smart Insole for Detecting Vertical Ground Reaction Force (vGRF) in Gait Analysis. *Sensors* **20**(4) (2020). <https://doi.org/10.3390/s20040957>, <https://www.mdpi.com/1424-8220/20/4/957>
14. UK National Health System: Physical activity guidelines for older adults, <https://www.nhs.uk/live-well/exercise/physical-activity-guidelines-older-adults/>, last accessed 11 Sep 2020